RSC Applied Polymers

ROYAL SOCIETY OF CHEMISTRY

PAPER

View Article Online
View Journal | View Issue

Cite this: *RSC Appl. Polym.*, 2025, **3**, 820

Black and purple metal-like lustrous films from anion-doped poly(3-alkoxyselenophene) dyes†‡

Satoru Tsukada, * Masatsugu Doi, Kan Nogami and Katsuyoshi Hoshino

Received 14th November 2024,
Accepted 28th March 2025

DOI: 10.1039/d4lp00338a

rsc.li/rscapplpolym

Materials that exhibit metallic luster without containing metals are promising alternatives to existing metallic paints and coatings. In this study, we successfully synthesized four types of anion-doped poly(3-alkoxyselenophene) and used them to develop metal-free metal-like lustrous films. By employing polyselenophene, we achieved the expression of luxurious glossy colors such as black and purple, which were difficult to obtain with previously reported polythiophene-based materials. The developed films were thoroughly investigated through reflectance spectroscopy, colorimetry, gloss measurements, and XRD analysis. The glossy colors exhibited by the polyselenophene films are suggested to arise from a well-balanced presence of face-on and edge-on lamellar crystals within the coated films, in addition to the optical properties of the polymer itself. The developed metal-like lustrous films do not contain any metals, being highly promising for applications in essential everyday items such as writing instruments, cosmetics, anti-counterfeiting inks, and automotive paints.

Introduction

Metallic and metal-like lustrous colors are deeply rooted in our society, culture, and religion as symbols of luxury and novelty. Therefore, they are widely applied in the exterior and interior of automobiles, aircrafts, and buildings.

The origin of luster in bulk metals is attributed to free electrons. At the same time, structural colors are produced by the reflection of light from periodic microstructures commonly observed in insects and birds.[1,2] Metallic luster paints containing metallic flakes, such as aluminum and zinc, are commonly used in everyday life.[3,4] The size of these flakes varies from a few to several tens of micrometers, with thicknesses ranging from less than 0.1 to 1 μm, facilitating the creation of attractive luster colors.[3,4] However, the use of metal flakes exhibits certain drawbacks, including susceptibility to corrosion, color migration, increased weight of the paint, and electromagnetic shielding issues.[3–5] Additionally, metal flakes can contribute to environmental pollution.[4,6–8]

The development of metal-free organic materials to create a metallic luster is highly promising in the field such as plating and polymers.[9–29] Compounds such as pyrrole,[11–16] polyaniline,[17,21] porphyrin,[23,30] azobenzene,[18,20,21,24,29,31,32] stilbene,[25] polyacetylene,[10,26] diarylethene,[27] and indole squaraine[28] derivatives have been reported to exhibit such luster. Furthermore, some of these compounds can change their gloss color when exposed to external stimuli,[27,29,31] while others are soluble in solvents, allowing the preparation of films. However, it is important to note that most of these compounds develop their gloss color in the bulk or crystalline state.

We previously demonstrated a coating film of an anion-doped poly(3-alkoxythiophene), synthesized *via* chemical oxidative polymerization, exhibiting a metal-like luster similar to gold and copper luster.[33–42] Such polythiophenes can be easily prepared as a coating solution using solvents with high polarity and afford metal-like luster films. Furthermore, films prepared *via* electrochemical polymerization also exhibit a gold-like luster.[43,44] Previous studies revealed that the existence of highly dense edge-on lamellar crystals causes a high refractive index and extinction coefficient, thus affording a metal-like luster. The development of materials with a higher reflectance that exhibit various luster colors is important for scientific research and practical applications.

So far, only thiophene derivatives have been employed to develop such films. Heterocyclic compounds containing other elements could be potentially used to fabricate metallic-tone glossy films with different properties from those of thiophene derivatives. Therefore, in this study, we focused on selenophene, a high-period analog of thiophene with a smaller HOMO–LUMO gap than thiophene. Polymers containing selenophene have been studied as electronic materials.[45–47] Compared to polythiophene, polyselenophene has a rigid

Department of Materials Science, Graduate School of Engineering, Chiba University, Inage-ku, Chiba 263-8522, Japan. E-mail: tsukada@chiba-u.jp

†This paper is dedicated to Emeritus Professor Takayuki Kawashima on the occasion of his 77th birthday ("Kiju" in Japanese).

‡Electronic supplementary information (ESI) available. See DOI: https://doi.org/10.1039/d4lp00338a

main chain backbone owing to its stronger quinoid properties and resistance to torsion.[47] In addition, a selenium atom has the same degree of electronegativity as a carbon atom and higher atomic radius and polarizability than a sulfur atom, which lead to a larger atomic refractive index in the Lorentz–Lorenz equation; therefore, a higher refractive index is expected.[48–51] These characteristics of (poly)selenophene are expected to afford films with a different color tone from that of polythiophene films. In this study, we developed metallic glossy materials based on anion-doped poly(3-alkoxyselenophene). The use of selenophene afforded a different luster color, significantly different from the typical color of thiophene-based materials, thereby opening new possibilities for material design and applications.

Experimental

The detailed experimental procedures for the synthesis of the selenophene monomers are available in the ESI‡ together with the reagents used.

Synthesis of ClO_4^--doped poly(3-methoxyselenophene) (MeOSe_ClO_4)

A solution of 3-methoxyselenophene (0.16 g, 1.0 mmol) in acetonitrile (10 mL) was bubbled with N_2 gas for 30 min. A solution of $Fe(ClO_4)_3{\cdot}nH_2O$ (1.10 g, 2.0 mmol) in acetonitrile (10 mL) was prepared *via* ultrasonication for 20 min and was added to the 3-methoxyselenophene/acetonitrile solution. The resulting mixture was stirred at room temperature for 1 h under a N_2 flow. The reaction mixture was filtered through a membrane filter (pore size = 0.1 μm), and the filter cake was thoroughly washed several times with methanol. The residue was vacuum-dried at 50 °C for 1.5 h to yield **MeOSe_ClO_4** as a black powder (0.17 g).

Synthesis of ClO_4^--doped poly(3-butoxyselenophene) (BuOSe_ClO_4)

BuOSe_ClO_4 was synthesized using 3-butoxyselenophene (0.19 g, 1.0 mmol) instead of 3-methoxyselenophene following the same procedure followed for **MeOSe_ClO_4** with slight modifications. The reaction mixture was filtered through a membrane filter (pore size = 0.1 μm), and the filter cake was thoroughly washed several times with ethanol. The residue was vacuum-dried at 50 °C for 1.5 h to yield **BuOSe_ClO_4** as a black powder (0.18 g).

Synthesis of BF_4^--doped poly(3-methoxyselenophene) (MeOSe_BF_4)

MeOSe_BF_4 was synthesized using $Cu(BF_4)_2{\cdot}nH_2O$ (0.70 g, 2.0 mmol) instead of $Fe(ClO_4)_3{\cdot}nH_2O$, following the same procedure as for **MeOSe_ClO_4**. **MeOSe_BF_4** was obtained as a black powder (0.15 g).

Synthesis of BF_4^--doped poly(3-butoxyselenophene) (BuOSe_BF_4)

BuOSe_BF_4 was synthesized using 3-butoxyselenophene (0.19 g, 1.0 mmol) instead of 3-methoxyselenophene following the same procedure as for **BuOSe_ClO_4**. **BuOSe_BF_4** was obtained as a black powder (0.17 g).

Coating solution and film preparation

The coating solutions were prepared by dissolving each polymer in propylene carbonate to 2 wt%, followed by stirring at room temperature for 3 h. The resulting solution was aged overnight. Then, 100 μL of the coating solution was deposited onto a 15 mm × 25 mm glass substrate using a micropipette and dried under hot air for 4 h at 60 °C to form a film.

Characterization

To determine the molecular weights of polymers, gel permeation chromatography (GPC) was performed using a solution of *N*-methyl-2-pyrrolidone containing 0.01 M LiBr with two Shodex KF-806 M columns and a UV-4075 system (JASCO Corporation). Each sample was dedoped by adding with 4 mL of *N*-methyl-2-pyrrolidone containing 0.01 M LiBr to polymer (1 mg), followed by stirring for 2 h and soaking in a hot water bath (50 °C) for 1 h. The measurements were performed at a flow rate of 0.9 mL min^{-1} and 60 °C, while the elution was monitored based on the absorbance at 273 nm. The molecular weight distribution curve obtained from the GPC measurements encompasses both the non-aggregated and π-dimer states. Therefore, the primary peak (M_p) indicates the molecular weight and can be used to compare the properties of polymers, with M_p reflecting the properties of the non-aggregated polymers. The molecular weight distribution curves were fitted *via* double Gaussian analysis with OriginPro2024 software (OriginLab Corp.) and our previously reported method.[39,42] Thermogravimetric-differential thermal analysis (TG-DTA) was performed using a DTG-60H (SHIMADZU CORPORATION). Sample was heated to 500 °C for **MeOSe_ClO_4** and **BuOSe_ClO_4**, to 200 °C for **MeOSe_BF_4** and **BuOSe_BF_4**, at the rate of 10 °C min^{-1} under N_2 flow. The UV-vis absorption spectra of the diluted coating solution were obtained using a Hitachi U-3000 spectrophotometer with a polymer content of 0.0020 wt%. The viscosities of the coating solutions were measured using a Brookfield LVDV-II + PCP cone- and plate-type rotoviscometer (Brookfield Eng. Lab.). During the viscosity measurements, the temperature was kept constant at 25.0 °C by circulating thermostated water (EYELA, cooling thermo pump CTP-101) in a jacketed vessel containing the solution. The polymer films were captured using a digital camera (EOS Kiss X8i, Canon) and digital microscope (VHX-5000, KEYENCE). The film thickness and root mean square surface roughness (R_q) were determined *via* laser-scanning microscopy (VK-9700, KEYENCE). The UV-vis reflectance spectra were obtained using a JASCO MSV-370 spectrometer with incidence and reflection angles of 23°. A vacuum-evaporated aluminum film (accessory of the spectrometer) was used

as a reference. The film color was assessed based on the CIE Lab values, with a^* representing redness–greenness and b^* representing yellowness-blueness. These values and diffuse reflectance spectra were obtained using a colorimeter (CM-600d, Konica Minolta) with a D65 illuminant and an observation angle of 10° (CIE 1964 Standard Observer). The optical constants of the films were determined using a variable-angle ellipsometer (Alpha-SE, J.A. Woollam Co.) at incidence angles of 65°, 70°, and 75° relative to a vertical line. The ellipsometry data were analyzed using J.A. Woollam CompleteEASE software version 6.37. The electric conductivity of the films was determined by measuring the sheet resistance *via* the two-terminal method using a resistivity meter (Hiresta-UX MCP-HT800 with a URS probe MCP-HTP14, Mitsubishi Chemical Analytech). The Se, F, and Cl contents in the polymer films were measured *via* scanning electron microscopy (SEM; JSM-6510A, JEOL) with energy-dispersive X-ray spectrometry (EDX) and were used to calculate the polymer doping level (number of dopant anions per thiophene ring unit). The X-ray diffraction patterns were recorded using an X-ray diffractometer (X'Pert MRD, Malvern Panalytical) at an in and out-of-plane configuration using a $2\theta/\omega$ scan mode and a Cu Kα source (λ = 1.5406 Å, 45 kV, 40 mA). The optical system module of the device used a Fixed Divergence Slit + 1/8° divergence slit on the incident side and a Det3 parallel plate (parallel plate collimator + graphite monochromator). The hardness of the films was measured according to the JIS-K5600-5-4 standard using a pencil hardness tester (BEVS 1301/750, Allgood Co. Ltd), where a pencil lead of various hardness grade (Hi-uni 9B–9H, Mitsubishi Pencil Co., Ltd) was used as the scratch stylus. A 750 ± 10 g load was applied to the film and the hardest pencil grade that did not damage the film was defined as the pencil hardness of the film.

Results and discussion

Preparation of polyselenophenes and their coating films

In this study, we synthesized two types of selenophene monomers with methoxy or *n*-butoxy groups as substituents at the 3-position on the selenophene ring. ClO_4^--and BF_4^--doped polymers were successfully synthesized *via* chemical oxidative polymerization using $Fe(ClO_4)_3{\cdot}nH_2O$ or $Cu(BF_4)_2{\cdot}6H_2O$ as an oxidant, respectively (Scheme 1). Polymerization was conducted following our previously reported method with slight modifications.[33,42] The four polymers were named **MeOSe_ClO$_4$**, **BuOSe_ClO$_4$**, **MeOSe_BF$_4$**, and **BuOSe_BF$_4$** for each side chain and dopant combination. The molecular weights of the polymers are summarized in Table 1. The molecular weight distribution curve obtained *via* GPC measurements encompassed both the non-aggregated and π-dimer states, following the same trend as our previously reported anion-doped poly(3-alkoxythiophene)s.[39,42] Therefore, the primary peak (M_p) indicates the molecular weight, which can be used to compare the properties of polymers, with M_p reflecting the properties of the non-aggregated polymers.[39,42] M_p ranged from 1080 to 1240, and the degree of polymerization (DP_p) suggested that all polymers comprised 6–7 monomers, with no significant variation. DP_p of polyselenophenes was slightly smaller than that of our previous polyalkoxythiophenes (DP_p: 8–12). Compared to polythiophenes, polyselenophenes are known to have a rigid main chain that is less likely to twist. Therefore, it is expected that the solubility of polyselenophenes is lower than that of polythiophenes. In our method, polyselenophenes were obtained as a precipitate after polymerization in acetonitrile. Polyselenophenes exhibit a lower solubility in acetonitrile compared to polythiophenes; it was therefore assumed that they were precipitated with a low degree of polymerization.

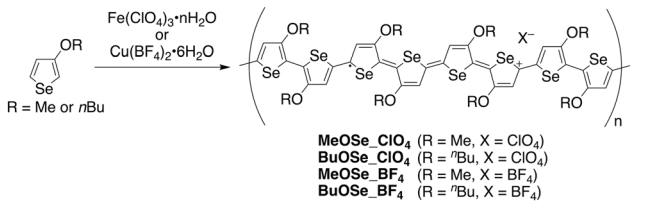

Scheme 1 Synthesis of the anion-doped poly(3-alkoxyselenophene) *via* chemical oxidative polymerization.

The doping level of each polymer was calculated *via* SEM-EDX analysis (Table 1). The doping level of polymers except for **BuOSe_BF$_4$** was approximately 20%, which is lower than that of the alkoxythiophene polymers (approximately 30%).[42] This is because the molecular weight of these polyselenophenes is small, and the doping level is also relatively small.

To investigate the regioregularity of polyselenophenes, we attempted to perform ^{1}H NMR measurements using the method from our previous study.[37] Our previous polythiophenes could be dedoped in DMSO-d_6 solution, and their NMR spectra could be measured after de-doping. However, the dedoped polyselenophenes were not soluble in DMSO-d_6 or other deuterated solvents. Therefore, ^{1}H NMR measurements could not be performed.

We have carried out TG-DTA measurements for all the polymers to investigate their thermal stability. TG-DTA curves are provided in the ESI as Fig. S5.‡ No significant weight loss was observed up to 200 °C. The values of 5% weight loss (T_{d5}), one of the indicators of thermal stability, are summarized in Table S3.‡ We note that ClO_4^--doped polymers were measured to 200 °C due to the possibility of rupture caused by ClO_4^- ions.

The preparation of the coating solution and films was attempted using **MeOSe_ClO$_4$**. First, the coating solution of **MeOSe_ClO$_4$** was prepared as a 1 wt% coating solution using nitromethane as the solvent, following the same procedure as that of the previous polyalkoxythiophene coating solution that afforded a metal-like lustrous coating film. However, the **MeOSe_ClO$_4$** powder produced residues in acetonitrile, which did not completely dissolve, and the coating film did not exhibit a lustrous effect. The glass substrate was covered with the polymer powder (Fig. S5‡). Conversely, **MeOSe_ClO$_4$** was

Table 1 Summary of the molecular weights and film properties of the anion-doped poly(3-alkoxyselenophene)s

Polymer	M_p [a]	DP_p [b]	Doping level[c] (%)	Film thickness[d] (mm)	R_q [d] (μm)	σ [e] (S cm^{-1})	Pencil hardness
MeOSe_ClO$_4$	1110	7	20	2.19	0.03	1.4×10^{-5}	2B
BuOSe_ClO$_4$	1210	6	21	2.21	0.03	1.4×10^{-7}	2B
MeOSe_BF$_4$	1080	7	18	2.57	0.02	2.7×10^{-4}	2B
BuOSe_BF$_4$	1240	6	28	2.11	0.04	1.2×10^{-6}	B

[a] Molecular weight corresponding to the main peak in the differential molecular weight distribution curve. [b] Polymerization degree calculated from M_p. [c] Determined *via* SEM-EDX analysis. [d] Determined *via* CLSM. [e] The electric conductivity of films was determined by measuring the sheet resistance *via* the double ring method using a resistivity meter.

completely dissolved in propylene carbonate and the coating film prepared from the propylene carbonate coating solution exhibited a metal-like lustrous effect. Details on the glossy color of the film will be provided later.

Fig. 1 shows photographs of the polyselenophene coating films, which were prepared using propylene carbonate as the solvent. The images were captured using a digital camera. All films reflected the scale of a stainless-steel ruler positioned perpendicular to the film surface, exhibiting a high luster. The surface of each film was observed with laser scanning microscopy (Fig. S7‡). The film thickness ranged from 2 to 3 μm, with all films exhibiting a relatively flat surface morphology and low root-mean-square roughness (R_q) of approximately 0.03 μm (Table 1). The electrical conductivity of polyselenophenes was 10^{-4} to 10^{-7}, which was almost the same as that of general π-conjugated organic polymers. Additionally, the electrical conductivity of **BuOSe_ClO$_4$** and **BuOSe_BF$_4$**, which have long alkoxy chain, was low. This trend is in agreement to that of polyalkoxythiophenes observed in our previous study.[42] This may be attributed to the alkoxy chain acting as an insulator that is separating the conductive main chains.[52] Moreover, when the alkoxy chain length was the same, the electric conductivity was higher for the BF_4^- dopant than for the ClO_4^- dopant, even though it had the same doping level. This finding will be further discussed below, together with the XRD crystal structure analysis of the coating films.

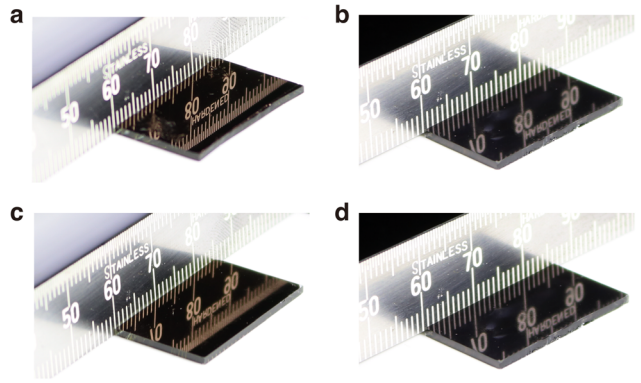

Fig. 1 Photographs of the (a) **MeOSe_ClO$_4$**, (b) **MeOSe_BF$_4$**, (c) **BuSe_ClO$_4$**, and (d) **BuOSe_BF$_4$** coating films prepared from propylene carbonate coating solutions of the corresponding polymer.

Furthermore, no significant difference in pencil hardness was observed between the polyalkoxyselenophene and poly(3-methoxythiophene) films (Table 1 and Table S3‡).

Optical properties of coating films

The coating films of **MeOSe_ClO$_4$** and **MeOSe_BF$_4$**, which have a methoxy group, exhibited a reddish-purple metallic luster (Fig. 1). The coating films of **BuOSe_ClO$_4$** and **BuOSe_BF$_4$**, which have a butoxy group, exhibited a black and purplish metallic luster, respectively. The glossy colors of the polyselenophene films differed from those of the ClO_4^--doped poly(3-methoxythiophene) film (**MeOT_ClO$_4$**) and poly(3-butoxythiophene) film that exhibited gold and copper-like lustrous, respectively.

Our previous studies on polyalkoxythiophenes were conducted using nitromethane as the solvent. Conversely, a coating solution of polyselenophenes was prepared using propylene carbonate. For comparison, a coating solution was prepared using the same solvent in the **MeOT_ClO$_4$**, and a film was prepared. The **MeOT_ClO$_4$** coating film exhibited a gold-like lustrous color (Fig. S8‡). More information regarding **MeOT_ClO$_4$** is provided in the ESI.‡

Spectral colorimetry was employed to evaluate the polymer film reflection color quantitatively. Fig. 2a shows the L^*, a^*, and b^* coordinates in the $L^*a^*b^*$ color space for all the polymer films, with the vacuum-evaporated metallic gold and copper films as the reference for comparison. The a^* and b^* values of all the polyselenophene films were closer to the origin than those of the vacuum-evaporated metallic gold and **MeOT_ClO$_4$** film (Fig. S9a‡). The a^* and b^* values of all polyselenophenes were located at 0 to 11 and −3 to 7, respectively (Table S4‡). The films containing a methoxy group exhibited larger a^* and b^* values than those with a butoxy group. In the $L^*a^*b^*$ color space, a higher a^* means more red components, whereas a higher b^* means more yellow components. The **BuOSe_ClO$_4$** and **BuOSe_BF$_4$** films were located close to their origin of the $L^*a^*b^*$ color space. Whereas, the **MeOSe_ClO$_4$** and **MeOSe_BF$_4$** films exhibited more reddish and yellowish tones and a reddish-purple luster.

The color lightness (L^*) of all polyselenophene films was 20–30, whereas that of **MeOT_ClO$_4$** was almost 40. In contrast, the L^* values for the evaporated gold and copper films were 80–90.

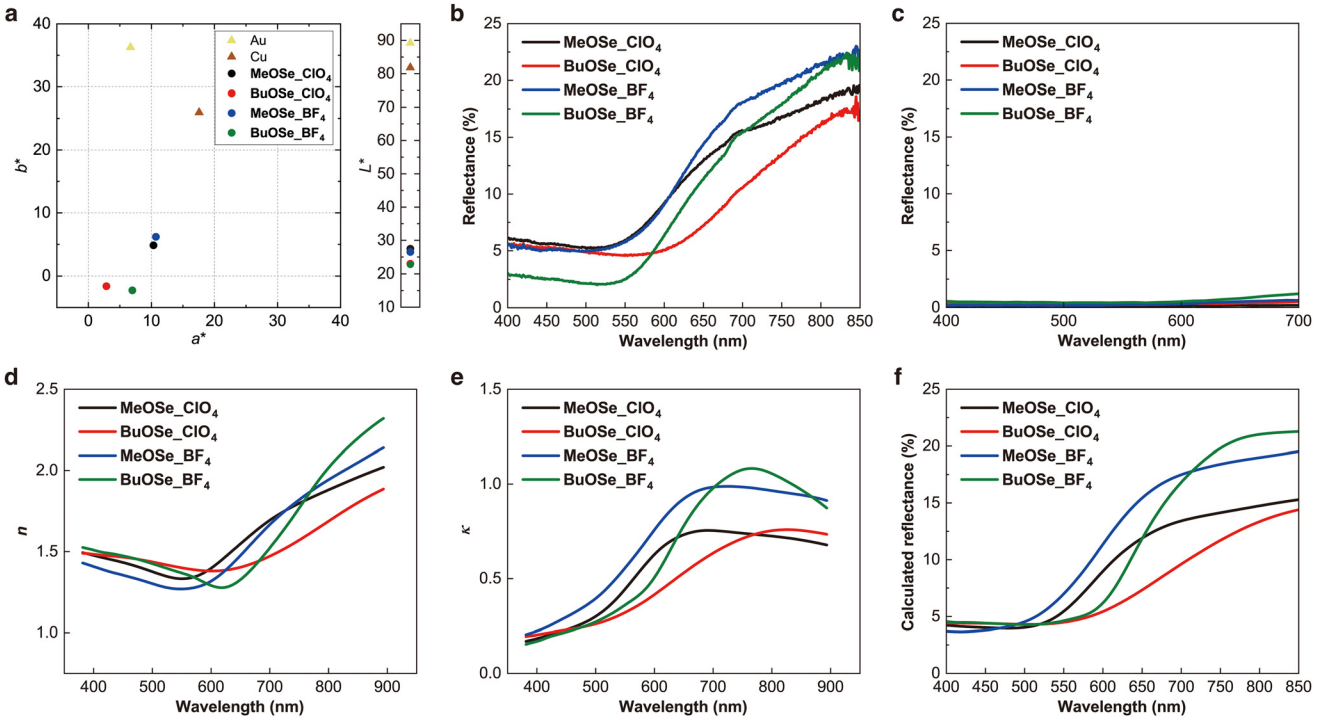

Fig. 2 (a) Values of a^*, b^*, and L^* according to a CIELab color system of anion-doped poly(3-alkoxyselenophene) films with the vacuum-evaporated gold and copper films. (b) Specular reflection, (c) diffuse reflection (d) refractive index (n), (e) extinction coefficient (κ), and (f) calculated reflection spectra of the anion-doped poly(3-alkoxyselenopehen) films.

The lustrous properties of the polymer films were evaluated *via* specular reflection spectrometry (Fig. 2b). The small reflection peak at approximately 690 nm was due to switching the light source and does not have a substantial reflection. The specular spectrum of all polyselenophenes exhibited a red-shift relative to that of **MeOT_ClO$_4$** (Fig. S9b‡). The polyselenophene films exhibited a strong reflection of red light (620–750 nm), a slightly strong reflection of orange (590–620 nm), and a lower reflection of purple (380–450 nm), blue (450–495 nm), green (495–570 nm), and yellow (570–590 nm) regions. Therefore, it was concluded that compared with **MeOT_ClO$_4$**, the polyselenophene films had a lower reflectance, especially in the green region, with the color of the film being closer to reddish-purple or black. The reflectance of the **MeOSe_BF$_4$** and **BuOSe_BF$_4$** films reached 20%, which is 5% higher than those of the **MeOSe_ClO$_4$** and **BuOSe_ClO$_4$** films. This may be attributed to the high crystallinity of the **MeOSe_BF$_4$** and **BuOSe_BF$_4$** films (more details on the XRD analysis section).

The diffuse reflection spectra were flat and demonstrated almost no reflectance values for all films (Fig. 2c), which are characteristics of the metallic luster.

In our previous study, we reported that the polyalkoxythiophene films exhibit gloss owing to their higher optical constants (refractive index (n) and extinction coefficient (κ)) compared to general transparent polymers. For instance, the n values of commercially available transparent polymers range from 1.3 to 1.7, exhibiting no photoabsorption in the visible region (*i.e.*, $\kappa = 0$)[53] and no metallic reflection. Our anion-doped poly(3-alkoxythiophene) films exhibited strong lustrous, unlike transparent resins, owing to the large n and κ values of organic materials in the visible region.[36,38,39,42] This is a characteristic of organic materials that develop metallic glosses. The optical constants of the polymer films were measured using ellipsometry to investigate the mechanism of luster appearance. Generally, the reflectance and chromaticity of a material are determined by the magnitude and wavelength dependence of the optical constants. In the case of normal incidence, the reflectance (R) between air and a given medium is related to n and κ, following eqn (1).[21]

$$R = \frac{(n-1)^2 + \kappa^2}{(n+1)^2 + \kappa^2} = 1 - \frac{4n}{(n+1)^2 + \kappa^2} \quad (1)$$

Fig. 2d–f show the n, κ, and R values obtained using eqn (1). The refractive index of the polyselenophene films is constant from 400 to 600 nm, being higher than that of the **MeOT_ClO$_4$** film. Then, after 600 nm, it increases. The reflectance rise wavelength of the polyselenophene films is red-shifted compared to that of the **MeOT_ClO$_4$** film. The refractive index in the long wavelength region was approximately 2, which is higher than that of general transparent resins and as high as that of metallic glossy materials comprising organic compounds.

π-Conjugated polymer incorporating a porphyrin unit (porphyrin film) that exhibits green metal-lustrous effects exhibit a

κ_{max} value of 2–3.[23,30] The κ_{max} of the polyaniline analogs containing an azobenzene unit that exhibits green metal-lustrous effects is approximately 2.3.[21] The extinction coefficient gradually increases from 400 nm, followed by a drastic increase from 550 nm, and becomes almost constant from ~700 nm. The calculated refraction spectra of the polyselenophene films were red-shifted compared to those of the polyalkoxythiophene films (Fig. 2f). Such findings are in agreement with the specular reflection spectra (Fig. 2b).

Our previous studies concluded that the glossy appearance of anion-doped polythiophene films was attributed to the compact lamellar crystallites formed by the polyalkoxythiophene chains in the film (more information is provided in the discussion on XRD Analysis).[33–42] In the anion-doped polyalkoxyselenophene films of this study, these crystallites also exhibited very large optical constants, as shown in Fig. 2d and e. Although the specular refraction spectra of the polyselenophene films and the vacuum-deposited metal film appear similar, the n and κ characteristics and mechanisms that produce the reflections differ. Therefore, the luster color of the poly(3-alkoxyselenophene) films was not caused by Drude's metallic response, which involves the screening of electromagnetic waves by free electrons; it was induced by the same mechanism observed in the thiophene polymer films.

Polymer orientation in the lustrous film

The formation of edge-on lamellar crystals within the film was attributed to the high refractive index and extinction coefficient of the developed polythiophene-based films (Fig. 3a). XRD measurements were performed to investigate the orientation of polyselenophenes in the coating film (Fig. 3b), revealing two peaks. The low-angle peak indicates the presence of edge-on lamellar crystals and its position varied according to the length of the side chains. That is, polymers with a methoxy group exhibited a peak at 2θ = 7–8°, while those with a butoxy group showed a peak at 2θ = 5–6°. The lamellar interlayer distance (a) was calculated from these peak positions. This distance increased by approximately four carbon atoms from **MeOSe_ClO$_4$** (1.12 nm) and **MeOSe_BF$_4$** (1.16 nm) to **BuOSe_ClO$_4$** (1.54 nm) and **BuOSe_BF$_4$** (1.51 nm) (Table S5‡). The difference of these values is comparable to our previously reported results for anion-doped poly(3-methoxythiophene) (1.13 nm) and poly(3-butoxythiophene) (1.52 nm),[42] with no change in the interlayer distance due to elemental differences in sulfur and selenium. The heavy atom substitution from the S element to the Se element does not result in significant variation in these distances; the lamellar spacing appears to be governed by the alkoxy chain.[54] This difference of 0.1 nm is relatively small compared to the wavelength of the visible light. Such a finding suggests that the observed gloss in polyselenophenes (similarly to polythiophenes) is not a structural color caused by the interference of periodic multilayers of approximately the wavelength of visible light.

The high-angle peak observed at approximately 2θ = 25° was attributed to the face-on lamellar crystals (Fig. 3c), and was independent of the dopant type and side chain. Such a finding indicates that the stacking distance is the same for all the tested polymers (*ca.* 0.36 nm). In previously reported polythiophenes with a liner alkoxy group, the amount of the face-on lamellar crystals was significantly lower compared to that of the edge-on lamellar crystals.[34–37,39,42] Conversely, the polyselenophenes developed in this study exhibit a distinct, broad peak in the high-angle region compared to the low-angle region. This suggests that the quantity of face-on lamellar crystals in polyselenophenes is greater than that observed in polythiophenes.

Our previously developed films with polythiophenes with a branched alkoxy group exhibited a dark color close to black.[42] Additionally, electrochemical methods can produce films where face-on lamellae dominate, resulting in a low-gloss red-purple color.[43] These results indicate that in polythiophenes with a branched alkoxy group, edge-on lamellar crystals are not completely formed, while edge-on and face-on lamellar crystals coexist in roughly equal amounts resulting in a low-gloss black-purple color. In contrast, polyselenophene films contain a higher proportion of edge-on lamellar crystals, which likely contribute to the observed higher brightness compared to the branched polythiophenes. This suggests that the edge-on lamellar crystals in polyselenophene are more effective at reflecting light, especially in the yellow and orange regions. Additionally, the face-on lamellar crystals contribute to a low-reflective black luster. The combination of these two

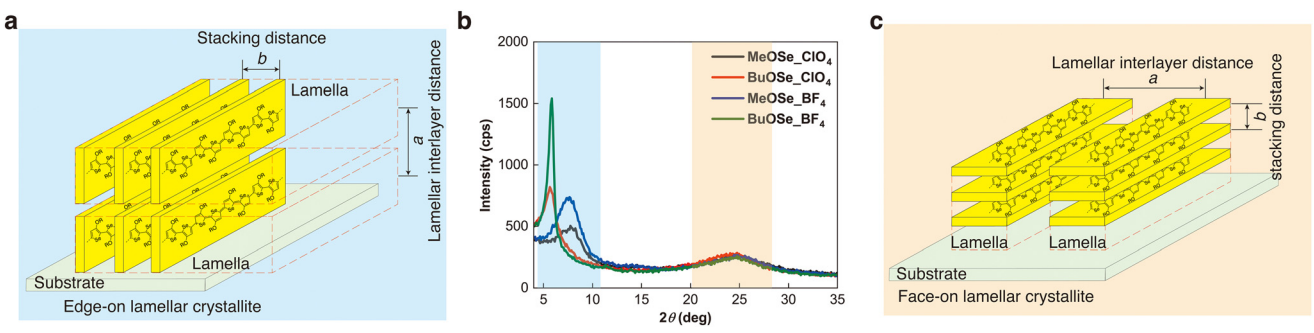

Fig. 3 (a) Structure of edge-on lamellar crystallites. (b) X-ray diffraction patterns of the anion-doped poly(3-alkoxyselenopehen) films. (c) Structure of face-on lamellar crystallites.

factors is thought to produce the exquisite, luxurious black and purple metallic gloss observed in the selenophene-based films.

Properties of the coating solution

Our previous investigations revealed that the orientation of polymers in the coating solution affects the properties of the coated film.[42] Ultraviolet–visible (UV-Vis) absorption measurements were conducted on the coating solutions. Fig. 4 and Fig. S11‡ show the UV-Vis absorption spectra of polyselenophenes and **MeOT_ClO$_4$** in a propylene carbonate solution, respectively. In the case of **MeOT_ClO$_4$**, peaks were observed at 640 (shoulder peak), 700, 770, and 860 nm, and were attributed to π-dimers, radical cations (polarons), or dications (bipolarons).[34] When nitromethane was used as the solvent, the obtained spectra exhibited an identical trend. Similar trends were also observed for all polyselenophenes, with little to no peak shifts. Assuming that the chemical species attributed to each peak are the same for polythiophenes and polyselenophenes, the spectra suggest that these species have the same effective conjugation length and electronic state. Generally, for the same degree of polymerization, the absorption spectra of polyselenophenes exhibit a red shift compared to those of polythiophenes. In this system, it is considered that no spectral shift was observed since the degree of polymerization of polyselenophenes is smaller than that of the corresponding polythiophenes.

Polymers composed of selenophene and tellurophene are known to form aggregates due to the interactions between the selenium or tellurium elements that make them up.[54–56] It is also known that such aggregates are less likely to form in thiophene-based systems. In the cases of **MeOSe_ClO$_4$** and **BuOSe_BF$_4$**, multiple peaks are observed in the region between 600 and 700 nm, suggesting the formation of multiple aggregation states. Other spectra exhibit broadening as shoulder peaks in this region; however, multiple aggregation states are believed to be present. These are thought to be aggregates formed due to Se–Se interactions. On the other hand, UV-vis measurements of the undiluted coating solution were performed, and a broadening of the spectra was observed for all the polymers. No significant spectral changes were observed due to differences in the side chain groups; however, a trend of varying peak positions was observed depending on the dopant. In other words, the peak top for ClO_4^--doped polymers appeared around 650 nm, whereas the peak top for BF_4^--doped polymers shifted to a higher wavelength region. This suggests that, in concentrated solutions, the dopant has a more significant influence on the formation of aggregates than the side chain groups. Additionally, UV-vis measurements of the dedoped polymers were also attempted; however, the dedoped polymers did not dissolve in propylene carbonate. To obtain more detailed information on the chemical species in the aggregated state, further investigations using dilution tests and theoretical calculations are considered necessary.

To investigate the stability of the coating solution, we conducted viscosity measurements (Fig. S12‡). The coating solution prepared using propylene carbonate showed no changes in viscosity, indicating a high stability. In contrast, the viscosity of the **MeOT_ClO$_4$** coating solution prepared using nitromethane is known to increase significantly within approximately one week.[34] Thus, the coating solution using propylene carbonate can be stored stably for an extended period. Notably, the coating solution prepared in propylene carbonate exhibited a higher initial viscosity compared to that prepared in nitromethane, which is attributed to the higher viscosity of pure propylene carbonate compared to nitromethane.

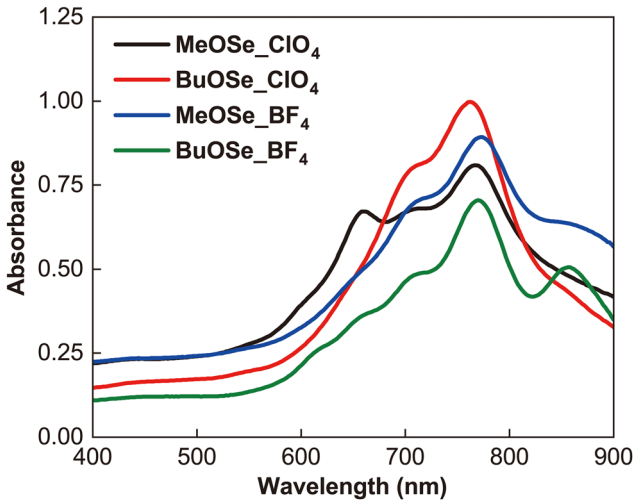

Fig. 4 Ultraviolet–visible (UV-vis) spectra of a diluted coating solution of anion-doped poly(3-alkoxyselenophene)s in propylene carbonate.

Conclusions

In this study, we successfully synthesized four anion-doped poly(3-alkoxyselenophene) derivatives with different side chains and dopant types. The obtained derivates were used to prepare glossy polyselenophene films exhibiting black, black-purple, and purple metallic lusters, which are perceived as luxurious and valuable colors. Such color tones were concluded to arise from a balanced presence of face-on and edge-on lamellar crystals within the coating films, in addition to the optical properties of the polymer itself. This glossy coloration is unique to polyselenophene and is currently difficult to achieve with polythiophene. Furthermore, the coating solutions exhibited high stability, allowing for long-term storage.

The metal-like lustrous films developed in this study do not contain any metals, similar to previously reported polythiophene-based materials. In the future, conducting light stability and durability tests will be important to support the claim that the oligomers in this study can serve as alternatives to conventional paints containing metals, being promising for applications in essential everyday items such as writing instruments, cosmetics, anti-counterfeiting inks, and automotive paints. Moreover, the presence of face-on and edge-on lamellar

crystals renders them suitable for applications in opto-electronic conversion devices (OPVs) and organic field-effect transistors (OFETs), for which further development is required.

Author contributions

S. T. conceived the idea, designed the experiments, and supervised the project. M. D. and K. N. conducted the majority of the experiments and analyzed the data. S. T. and K. H. instructed and aided the data analysis. S. T. wrote, edited, and revised the manuscript together with M. D., K. N. and K. H. All authors have given approval to the final version of the manuscript.

Data availability

The data supporting this article have been included as part of the ESI.‡

Conflicts of interest

The authors declare no competing financial interest.

Acknowledgements

This work was supported by JSPS KAKENHI (grant number JP21K05194 (S. T.)). This work was based on the results obtained from a project, JPNP20004, subsidized by the New Energy and Industrial Technology Development Organization (NEDO) (S. T.). This work was also supported by the Kato Foundation for the Promotion of Science and Iketani Science and Technology Foundation (S. T.).

References

1 M. D. Shawkey and L. D'Alba, *Philos. Trans. R. Soc., B*, 2017, **372**, 20160536.
2 I. C. Cuthill, W. L. Allen, K. Arbuckle, B. Caspers, G. Chaplin, M. E. Hauber, G. E. Hill, N. G. Jablonski, C. D. Jiggins, A. Kelber, J. Mappes, J. Marshall, R. Merrill, D. Osorio, R. Prum, N. W. Roberts, A. Roulin, H. M. Rowland, T. N. Sherratt, J. Skelhorn, M. P. Speed, M. Stevens, M. C. Stoddard, D. Stuart-Fox, L. Talas, E. Tibbetts and T. Caro, *Science*, 2017, **357**, eaan0221.
3 G. Pfaff and P. Reynders, *Chem. Rev.*, 1999, **99**, 1963–1982.
4 F. J. Maile, G. Pfaff and P. Reynders, *Prog. Org. Coat.*, 2005, **54**, 150–163.
5 R. Schoppe, *Aluminum Pigments for Plastics*, 2012.
6 N. Singh and A. Turner, *Mar. Pollut. Bull.*, 2009, **58**, 559–564.
7 S. L. Huang, C.-Y. Yin and S. Y. Yap, *J. Hazard. Mater.*, 2010, **174**, 839–842.
8 C. K. Takahashi, A. Turner, G. E. Millward and G. A. Glegg, *Mar. Pollut. Bull.*, 2012, **64**, 133–137.
9 B. G. Anex and W. T. Simpson, *Rev. Mod. Phys.*, 1960, **32**, 466–476.
10 H. Shirakawa, E. J. Louis, A. G. MacDiarmid, C. K. Chiang and A. J. Heeger, *J. Chem. Soc., Chem. Commun.*, 1977, 578–580.
11 K. Ogura, R. Zhao, H. Yanai, K. Maeda, R. Tozawa, S. Matsumoto and M. Akazome, *Bull. Chem. Soc. Jpn.*, 2002, **75**, 2359–2370.
12 R. Zhao, M. Akazome, S. Matsumoto and K. Ogura, *Tetrahedron*, 2002, **58**, 10225–10231.
13 R. Zhao, S. Matsumoto, M. Akazome and K. Ogura, *Tetrahedron*, 2002, **58**, 10233–10241.
14 K. Ogura, R. Zhao, M. Jiang, M. Akazome, S. Matsumoto and K. Yamaguchi, *Tetrahedron Lett.*, 2003, **44**, 3595–3598.
15 K. Ogura, R. Zhao, T. Mizuoka, M. Akazome and S. Matsumoto, *Org. Biomol. Chem.*, 2003, **1**, 3845–3850.
16 K. Ogura, K. Ooshima, M. Akazome and S. Matsumoto, *Tetrahedron*, 2006, **62**, 2484–2491.
17 M. Kukino, J. Kuwabara, K. Matsuishi, T. Fukuda and T. Kanbara, *Chem. Lett.*, 2010, **39**, 1248–1250.
18 A. Matsumoto, M. Kawaharazuka, Y. Takahashi, N. Yoshino, T. Kawai and Y. Kondo, *J. Oleo Sci.*, 2010, **59**, 151–156.
19 H. Goto, *J. Polym. Sci., Part A: Polym. Chem.*, 2013, **51**, 3097–3102.
20 Y. Kondo, A. Matsumoto, K. Fukuyasu, K. Nakajima and Y. Takahashi, *Langmuir*, 2014, **30**, 4422–4426.
21 H. Yamada, M. Kukino, Z. A. Wang, R. Miyabara, N. Fujimoto, J. Kuwabara, K. Matsuishi and T. Kanbara, *J. Appl. Polym. Sci.*, 2015, **132**, 41275.
22 C. T. Poon, D. Wu and V. W. Yam, *Angew. Chem., Int. Ed.*, 2016, **55**, 3647–3651.
23 M. Morisue, Y. Hoshino, M. Shimizu, S. Tomita, S. Sasaki, S. Sakurai, T. Hikima, A. Kawamura, M. Kohri, J. Matsui and T. Yamao, *Chem. Commun.*, 2017, **53**, 10703–10706.
24 S.-I. Lim, K.-H. Ryu, D.-Y. Jeon, C.-M. Yang, L. De Sio, D.-Y. Kim and K.-U. Jeong, *Cryst. Growth Des.*, 2020, **20**, 5896–5902.
25 N. Saito, M. Ono, H. Komatsubara, K. Fukushima, Y. Takahashi and Y. Kondo, *Dyes Pigm.*, 2020, **179**, 108394.
26 B. R. Boswell, C. M. F. Mansson, J. M. Cox, Z. Jin, J. A. H. Romaniuk, K. P. Lindquist, L. Cegelski, Y. Xia, S. A. Lopez and N. Z. Burns, *Nat. Chem.*, 2021, **13**, 41–46.
27 Y. Nakagawa, R. Nishimura, M. Morimoto, S. Yokojima, S. Nakamura and K. Uchida, *Bull. Chem. Soc. Jpn.*, 2022, **95**, 1438–1444.
28 S. Yamazaki, T. Okazaki, T. Murafuji, M. Sumimoto and Y. Mikata, *Langmuir*, 2024, **40**, 19722–19730.
29 K. Tachibana, Y. Kojima, H. Masu, N. Ichikuni, H. Takahashi, K. Akiyama, K. Nakamura, N. Kobayashi, S. Ichikawa, Y. Kondo, Y. Oaki, J. Matsui, S. Okada,

T. Omatsu, K. Kishikawa and M. Kohri, *ACS Appl. Mater. Interfaces*, 2024, **16**, 63904–63913.
30 M. Morisue, M. Kawanishi, Y. Miyake, K. Kanaori, K. Tachibana, M. Ohke, M. Kohri, J. Matsui, T. Hoshino and S. Sasaki, *Macromolecules*, 2023, **56**, 7993–8002.
31 Y. Kojima, K. Kishikawa, S. Ichikawa, J. Matsui, K. Hirai, Y. Kondo and M. Kohri, *ACS Appl. Polym. Mater.*, 2021, **3**, 1819–1827.
32 K. Onodera, N. Saito and Y. Kondo, *Chem. Lett.*, 2022, **51**, 485–488.
33 R. Tagawa, H. Masu, T. Itoh and K. Hoshino, *RSC Adv.*, 2014, **4**, 24053–24058.
34 Y. Takashina, T. Mitogawa, K. Saito and K. Hoshino, *Langmuir*, 2018, **34**, 3049–3057.
35 Y. Takashina and K. Hoshino, *Polym. J.*, 2019, **51**, 591–599.
36 M. Tachiki, R. Tagawa and K. Hoshino, *ACS Omega*, 2020, **5**, 24379–24388.
37 M. Kubo, H. Doi, R. Saito, K. Horikoshi, S. Tsukada and K. Hoshino, *Polym. J.*, 2021, **53**, 1019–1029.
38 M. Kubo, M. Tachiki, T. Mitogawa, K. Saito, R. Saito, S. Tsukada, T. Horiuchi and K. Hoshino, *Coatings*, 2021, **11**, 861.
39 M. Tachiki, S. Tsukada and K. Hoshino, *Dyes Pigm.*, 2021, **190**, 109302.
40 S. Sugiura, T. Mitogawa, K. Saito, R. Tamura, S. Tsukada, T. Horiuchi and K. Hoshino, *RSC Adv.*, 2022, **12**, 19965–19973.
41 R. Tamura, K. Miyamoto, S. Tsukada and K. Hoshino, *Mater. Adv.*, 2022, **3**, 3428–3437.
42 S. Tsukada, R. Saito and K. Hoshino, *ACS Appl. Opt. Mater.*, 2023, **1**, 1847–1855.
43 T. Tokuda and K. Hoshino, *Polym. J.*, 2016, **48**, 1141–1149.
44 D. Takamura and K. Hoshino, *Chem. Lett.*, 2018, **47**, 540–543.
45 A. Patra and M. Bendikov, *J. Mater. Chem.*, 2010, **20**, 422–433.
46 P. S. Hellwig, T. J. Peglow, F. Penteado, L. Bagnoli, G. Perin and E. J. Lenardao, *Molecules*, 2020, **25**, 5907.
47 S. Ye, V. Lotocki, H. Xu and D. S. Seferos, *Chem. Soc. Rev.*, 2022, **51**, 6442–6474.
48 J. K. Nagle, *J. Am. Chem. Soc.*, 1990, **112**, 4741–4747.
49 H. Kim, B.-C. Ku, M. Goh, H. C. Ko, S. Ando and N.-H. You, *Macromolecules*, 2019, **52**, 827–834.
50 Y. Tokushita, S. Furuya, S. Nobe, K. Nakabayashi, S. Samitsu and H. Mori, *Polymer*, 2021, **237**, 124346.
51 Y. Tokushita, A. Watanabe, A. Torii, K. Nakabayashi, S. Samitsu and H. Mori, *React. Funct. Polym.*, 2021, **165**, 104960.
52 K. Kaneto, W. Y. Lim, W. Takashima, T. Endo and M. Rikukawa, *Jpn. J. Appl. Phys.*, 2000, **39**, L872–L874.
53 J. Brandrup, E. H. Immergut, E. A. Grulke, A. Abe and D. R. Bloch, *Polymer handbook*, Wiley-Interscience, 4th edn, 1999.
54 R. S. Ashraf, I. Meager, M. Nikolka, M. Kirkus, M. Planells, B. C. Schroeder, S. Holliday, M. Hurhangee, C. B. Nielsen, H. Sirringhaus and I. McCulloch, *J. Am. Chem. Soc.*, 2015, **137**, 1314–1321.
55 M. Planells, B. C. Schroeder and I. McCulloch, *Macromolecules*, 2014, **47**, 5889–5894.
56 B. D. Paulsen, D. Meli, M. Moser, A. Marks, J. F. Ponder, R. Wu, E. A. Schafer, J. Strzalka, Q. Zhang, I. McCulloch and J. Rivnay, *Chem. Mater.*, 2024, **36**, 1818–1830.